Soft Matter

PAPER

Cite this: *Soft Matter*, 2022, **18**, 7510

A particulate blood analogue based on artificial viscoelastic blood plasma and RBC-like microparticles at a concentration matching the human haematocrit

A. Rubio,[a] M. López,[a] T. Rodrigues, [bc] L. Campo-Deaño [bc] and E. J. Vega *[a]

Received 15th July 2022,
Accepted 2nd September 2022

DOI: 10.1039/d2sm00947a

rsc.li/soft-matter-journal

There has been enormous interest in the production of fluids with rheological properties similar to those of real blood over the last few years. Application fields range from biomicrofluidics (microscale) to forensic science (macroscale). The inclusion of flexible microparticles in blood analogue fluids has been demonstrated to be essential in order to reproduce the behaviour of blood flow in these fields. Here, we describe a protocol to produce a whole human blood analogue composed of a proposed plasma analogue and flexible spherical microparticles that mimic the key structural attributes of RBCs (size and mechanical properties), at a concentration matching the human haematocrit (~42% by volume). Polydimethylsiloxane (PDMS) flexible microparticles were used to mimic RBCs, whose capability to deform is tunable by means of the mixing ratio of the PDMS precursor. Their flow through glass micronozzles allowed us to find the appropriate mixing ratio of PDMS to have approximately the same Young's modulus (E) as that exhibited by real RBCs. Shear and extensional rheology and microrheology techniques were used to match the properties exhibited by human plasma and whole blood at body temperature (37 °C). Finally, we study the flow of our proposed fluid through a microfluidic channel, showing the *in vitro* reproduction of the multiphase flow effects taking place in the human microcirculatory system, such as the cell-free layer (CFL) and the Fåhræus–Lindqvist effect. A macroscale application in the field of forensic science is also presented, concerning the impact of our blood analogue droplets on a solid surface for bloodstain pattern analysis.

1 Introduction

The use of human blood in fields from biomicrofluidics to forensic science complicates the scientific experimental studies due to diverse problems such as coagulation, sample storage and disposal, and ethical and economic issues.

Enormous interest in the production of fluids with physiological and rheological properties similar to those of real blood has been generated in the last few years to conduct *in vitro* experiments for biomedical applications at the microscale and macroscale [see Fig. 1(a)]. The development of blood analogues would allow *in vitro*-studies that would be very helpful in the design and testing of therapy strategies and medical devices to be performed.[1,2] Several liquid mixtures and solutions have been considered for mimicking blood, and lately, there have also been attempts to create particulate suspensions.[1] The addition of small sized flexible particles to blood analogues to mimic Red Blood Cells (RBCs) has been demonstrated to be essential to reproduce the multiphase effects taking place in a microcirculatory system, such as the cell-free layer (CFL) and Fåhræus–Lindqvist effect or even for drug delivery.[3] Moreover, other capabilities such as their ability to reproduce transport-oxygen properties or the necessity to mimic the surface charge of these cells have also been explored.[4]

In the forensic science field, although commercial blood simulants have been created for bloodstain pattern analysis (see Fig. 1b), the high rigidity of the microparticles used in their formulation hinders the accurate reproducibility of the behaviour of a simple blood droplet impacting onto a solid surface.[5] The capacity to deform (energy dissipation) the RBC-like microparticles seems to be the key to be able to reproduce more accurately the human blood spreading and splashing behaviour.[5]

Therefore, one of the key properties of the particles or capsules used to mimic RBCs is their deformability. The

[a] *Depto. de Ingeniería Mecánica, Energética y de los Materiales and Instituto de Computación Científica Avanzada (ICCAEx), Universidad de Extremadura, E-06006, Badajoz, Spain. E-mail: ejvega@unex*
[b] *CEFT, Depto. de Engenharia Mecânica, Faculdade de Engenharia, Universidade do Porto, Rua Dr. Roberto Frias, 4200-465, Porto, Portugal*
[c] *ALiCE, Faculdade de Engenharia, Universidade do Porto, Rua Dr. Roberto Frias, 4200-465, Porto, Portugal*

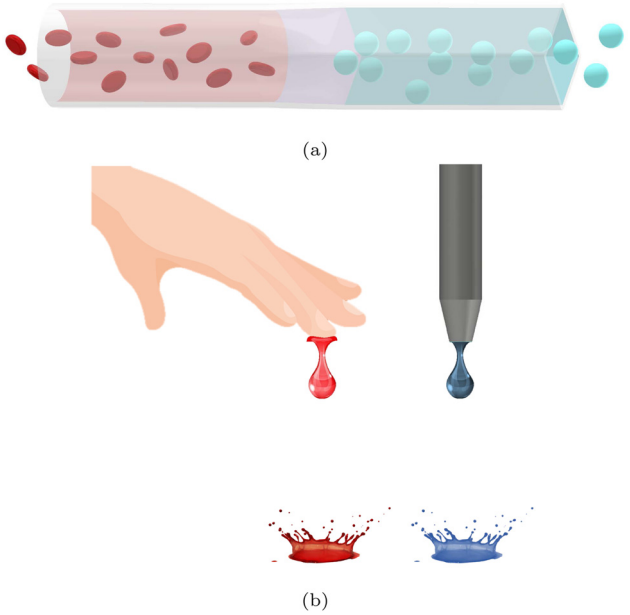

Fig. 1 Microfluidics as a platform to mimic and study blood flow in the human microcirculatory system (a). Bloodstain pattern analysis in forensic science (b).

deformation index DI and the elastic modulus E have frequently been used to evaluate it. Several attempts have been made to estimate the RBCs' elastic modulus, mostly using atomic force microscopy,[6–11] though it is not uniform over their surface.[6] It has been shown that the measured value depends on several aspects, such as the procedure to prepare the sample,[10] the sample storage time,[7] and even the particular blood donor.[6] For that reason, reported healthy RBCs mean that the elastic modulus ranges from 1 to 30 kPa. Polydimethylsiloxane (PDMS) microparticles are known to show very high deformability.[12–14] For this reason, they are good candidates to mimic RBCs' behavior. PDMS is produced from the mixture of two components: the siloxane base and the curing agent, and the resulting properties depend on the ratio of the precursors in the mixture.

In this paper viscoelastic fluids mimicking the non-Newtonian properties of real human plasma (shear viscosity and viscoelastic moduli) were carefully developed. The production and addition of flexible spherical PDMS microparticles that mimic the key structural attributes of RBCs (size and mechanical properties), in 42% by volume (similar to the human haematocrit), provided a new blood particulate analogue fluid. Shear and extensional rheology and microrheology techniques allowed us to match the properties exhibited by human plasma and whole human blood at body temperature. To evaluate the flow and mechanical properties of the particulate blood analogue fluid, the cell (particle) free layer (CFL/PFL) in a microfluidic channel with an important constriction (microstenosis) and the droplet impact for bloodstain pattern analysis were analysed at micro and macroscales, respectively.

2 Materials and methods

2.1 RBC-like PDMS microparticles

The two-syringe membrane emulsification technique (2SME)[13] was used for fabricating polydimethylsiloxane (PDMS) particles [see Fig. 2(a)]. First, we prepared a mixture of the siloxane base (Part A) and the curing agent (Part B) (Dow Corning SYLGARD 184 Silicone Elastomer) at the desired weight ratio (precursor to curing agent) and stirred it manually for ten minutes. Then, we loaded 1 ml of the PDMS precursor mixture into one syringe and 5 ml of distilled water with a surfactant (3 wt% sodium dodecyl sulfate, SDS) on the opposite. The addition of the surfactant prevents the sedimentation and flocculation of the particles. The emulsion was produced with five back and forth flow cycles through a 10 μm pore size filter. To cure the PDMS, we placed the emulsion on the heater with a standard magnetic stirrer at 70 °C for 3 hours, and then we waited for 24 hours for it to reach room temperature. The final particles proportion in the suspension was 1.65 ± 0.24 wt% (calculated by drying different samples).

For each deformation assessment, we prepared the particle solution and then modified the liquid phase by adding Dextran 40 (10 wt%) to use the same liquid phase as the RBC suspension (dextran is used to preserve the RBC properties) and rhodamine B to improve particle visualization in the experiments. The solution was injected through a fire-shaped nozzle[15] to evaluate the deformability of RBCs, and to compare it with that of PDMS particles produced with different

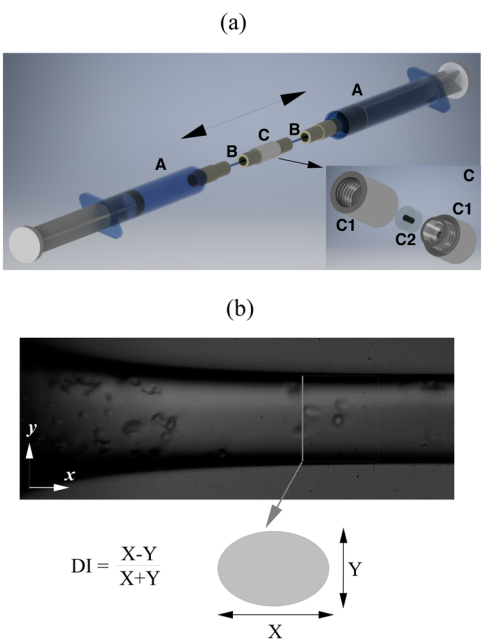

Fig. 2 (a) Elements of the two-syringe membrane emulsification technique (2SME) used to produce PDMS microparticles: two plastic syringes of 5 ml (A), tubing and connectors (B), and an inline filter/membrane (C) composed of a column (C1) and a frit (C2).[13] (b) Visualization of the microparticles flowing through a glass micronozzle (above) and deformation index (DI) definition (below).[13] Figures (a) and (b) reproduced from López *et al.*[13] with permission from Elsevier.

precursors ratios. We used a micronozzle with a neck diameter of 66 ± 3 μm and a flow rate Q of 5 μl min^{-1} and measured the deformation at the neck. The experimental setup used to observe the deformation of the flexible particles and cells while flowing along the nozzle was the same as that described in ref. 13.

For the RBC suspension preparation, a blood sample from a healthy donor was collected and ethylenediaminetetraacetic acid (2K EDTA) was added to prevent coagulation. The sample was stored hermetically at 4 °C and later centrifuged to separate the RBCs from the bulk blood. Then, RBCs were resuspended and washed with physiological salt solution (PSS) and centrifuged several times again. To maintain the cell homeostasis and avoid sedimentation, 1% by volume of healthy RBCs were redispersed by slow stirring in a 1 M solution composed of 5 g of Dextran 40 powders (Sigma-Aldrich), 7.35 ml of NaCl, 201 μl of KCl, and 68 μl of $CaCl_2H_2O$.[16–18]

The deformation index (DI) shown in Fig. 2(b) was used, where X is the length of the particle along the nozzle/capillary axis and Y the corresponding value in the normal direction. In each experiment, 100 particles/cells moving along the nozzle centerline (±5 μm) were measured when crossing a particular section (±33 μm). Fig. 2b also shows the measurement region at the neck section. The particle/cell dimensions were obtained manually at the pixel level, and Chauvenet's criterion was used to identify and reject outliers.

The RBCs in our experiments can be assumed to be aligned with the flow direction, *i.e.*, with the nozzle axis x (see Fig. 3). If the flow were perfectly axisymmetric, then the RBC orientation angle φ formed with the y axis would take values in the interval $[0,2\pi]$ with an equiprobable distribution. In this case, the mean value of the apparent particle length Y_{app} of RBCs randomly chosen is

$$\langle Y_{app} \rangle = \frac{1}{2\pi}\int_0^{2\pi} [(Y - 2R)\cos\varphi + 2R]\mathrm{d}\varphi. \quad (1)$$

Eqn (1) allows one to calculate Y from the value of $\langle Y_{app} \rangle$ measured in the experiment. The result differed by about 8% from the value measured with the method described above, which constitutes a consistency test for our measurements.

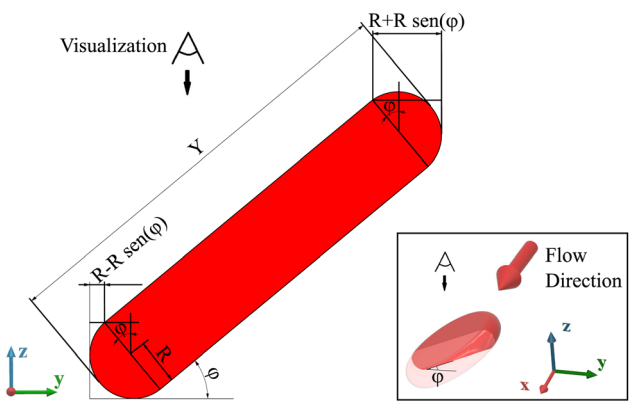

Fig. 3 Sketch of RBC visualization.

2.2 Formulation of the working fluids

Fig. 4 schematises the formulation of the different working fluids: a base Newtonian solution of 85 wt% water (W) and 15 wt% dimethyl sulfoxide (DMSO)[19] with the addition of 50 ppm polyethylene oxide (PEO) with different molecular weights M_w [600 kDa (PEO600K), 2 MDa (PEO2M), 4 MDa (PEO4M) and 8 MDa (PEO8M)] were prepared in order to confer the required viscoelasticity which mimics that of human blood plasma[20,21] (de-ionized water and PEO were purchased from Sigma Aldrich, and DMSO from Merck); a particulate viscoelastic fluid was prepared with the base solution and with the addition of the aforementioned PDMS microparticles at a concentration of roughly 42 wt%, *i.e.*, matching the human haematocrit (Hct), to reproduce the rheological behavior of whole human blood. It was confirmed that the blood analogue preserves the properties for about one month when it is properly stored in a fridge.

The density ρ of the tested fluids was measured with a pycnometer of 10 ± 1 ml and a precision balance. Table 1 shows the experimental results and the typical values of the density of human plasma[22] at 20 °C, and RBCs and whole blood[23] at 37 °C: 1027, 1095 and 1047 kg m^{-3}, respectively.

The surface tension γ, a relevant property for the droplet impact application presented in Section 3.6, was also measured using the Theoretical Interface Fitting Analysis (TIFA) method,[25] resulting in a value of 38 mN m^{-1} for the particulate viscoelastic fluid DMSO/W-PEO4M$_{45:1}$, near to the value of human blood of around 52 mN m^{-1} from the literature.[26,27] Steady shear, extensional rheology and microrheology experiments were used to compare the properties exhibited by human plasma and whole human blood with that of the working fluids.

2.3 Steady shear rheology

A stress-controlled rotational rheometer (Anton Paar Physica MCR 301) was used to obtain the steady shear viscosity, η, as a function of the shear rate, $\dot{\gamma}$ for all the fluid samples (Fig. 9). A plate–plate geometry (PP50) with a radius of R = 25 mm and a gap of h = 100 μm, was used to obtain reliable data in a wide range of shear rates. The temperature within the fluid volume was set at 20 °C and controlled by a Peltier cooling system. Steady-state viscosity curves were obtained from 1 to 10 000 s^{-1}. At least three independent measurements were performed to ensure the reproducibility of the results; trends were considered significant when means of the compared sets differed at $P < 0.05$ (Students t-test). The range of shear rate providing reliable data was set for each sample between the limit of the rheometer sensitivity (low-shear rate limit) and the onset of inertial instabilities (high-shear rate limit).[28]

It should be pointed out that although serrated plate–plate geometry was used to conduct steady shear rheology with suspensions in previous studies,[14,29] a protrusion flow (at high shear rates) can result in non reliable data.[30] Relatively low viscous suspensions should be analysed with geometries having smooth surfaces, plate–plate geometry.[30]

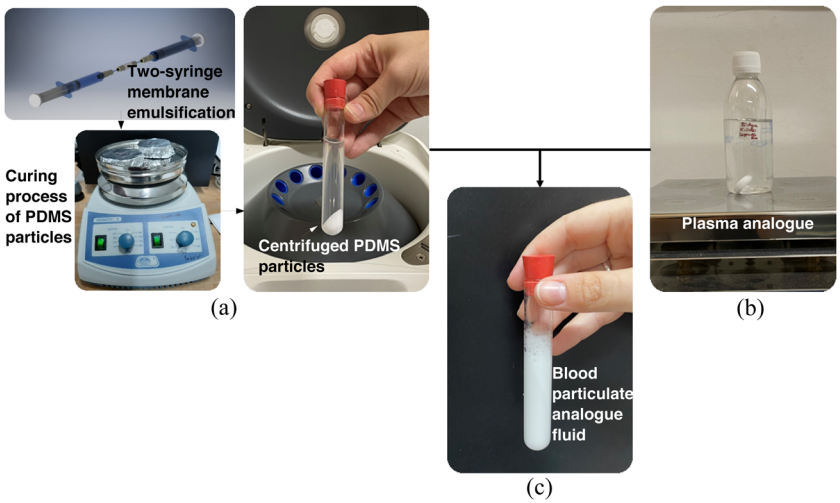

Fig. 4 (a) Production, curing and centrifugation of the suspension with PDMS microparticles (Section 2.1). (b) DMSO/water solution (15/85 wt%) with 50 ppm of PEO at different molecular weights M_w. (c) Particulate viscoelastic fluid (around 42 vol% of microparticles).

Table 1 Densities (ρ) of the working liquids, particles, and whole dispersions at 20 ± 2 °C (RBCs, and whole blood at 37 °C). The PDMS densities ρ for each mixing ratio were estimated from Hocheng *et al.*[24] The rest of the data came from the manufacturer or literature, or were obtained experimentally in the laboratory

	PEO			PDMS		
	M_w (kDa)	c (wt%)	DMSO[a] (wt%)	Ratio	"Hct"[b] (vol%)	ρ (k gm^{-3})
Blood plasma[22]	—	—	—	—	—	1026.6 ± 0.3
DMSO/W-PEO600K	600	0.005	15	—	—	1012.0
DMSO/W-PEO2M	2000	0.005	15	—	—	1012.8
DMSO/W-PEO4M	4000	0.005	15	—	—	1013.0
DMSO/W-PEO8M	8000	0.005	15	—	—	1013.0
RBCs[23]	—	—	—	—	—	1095 ± 2
PDMS 30 : 1	—	—		30 : 1	—	1050.0
PDMS 45 : 1	—	—	—	45 : 1	—	1050.0
PDMS 60 : 1	—	—	—	60 : 1	—	1050.0
Whole blood[23]	—	—	—	—	—	1047 ± 6
DMSO/W-PEO600K$_{45:1}$	600	0.005	15	45 : 1	42	1015.0
DMSO/W-PEO2M$_{45:1}$	2000	0.005	15	45 : 1	42	1015.0
DMSO/W-PEO4M$_{45:1}$	4000	0.005	15	45 : 1	42	1015.1
DMSO/W-PEO8M$_{45:1}$	8000	0.005	15	45 : 1	42	1015.3
DMSO/W-PEO8M$_{30:1}$	8000	0.005	15	30 : 1	42	1015.2
DMSO/W-PEO8M$_{60:1}$	8000	0.005	15	60 : 1	42	1015.3

[a] DMSO–water solution. [b] Microparticle volume fraction or, equivalently, "haematocrit" (Hct).

2.4 Extensional rheology

A custom-made capillary breakup extensional rheometer was used to obtain the extensional relaxation time λ_e, see Fig. 5(a), for all the working fluids. The experimental setup and procedure used for this purpose are described in detail in Sousa *et al.*[21,31] Briefly, a liquid bridge about 500 μm in length with the triple contact lines anchored to the edges of the supporting rods was formed, and filament thinning was induced by using the slow retraction method (SRM).[32] The subsequent filament thinning and breakup was recorded using a high speed camera (Photron, Fastcam SA5) up to 50 000 frames per second, as illustrated in Fig. 5(b). The particle sedimentation was insignificant during our extensional rheology experiments.

The images were processed to determine the filament diameter d with a sub-pixel resolution technique.[33,34] By plotting the diameter data as a function of time in a semi-log scale, one can straightforwardly identify the time interval within which the diameter decays exponentially. This interval corresponds to the elasto-capillary regime, where the balance between tensile stresses and surface tension produces the homogeneous stretching of a quasi-cylindrical thread. The time evolution of the filament diameter d in this regime was fitted using the exponential function[35]

$$d(t) = Ae^{-t/(3\lambda_e)}, \quad (2)$$

in order to calculate the extensional relaxation time λ_e. Each experiment was conducted five times to assess the reproducibility and to estimate the standard deviation.

2.5 Multiple particle tracking microrheology

Multiple particle tracking (MPT) microrheology was performed as previously described.[22] MPT is a passive microrheological technique in which the Brownian motion of probe particles is measured and related to bulk rheological properties using the generalised Stokes–Einstein relation (GSER) by

$$J(\tau) = \frac{3\pi a}{dkT}\langle \Delta r^2(\tau)\rangle, \quad (3)$$

where J is the creep compliance, τ is the lag time, kT is the thermal energy, d is the number of spatial dimensions, a is the probe radius and $\langle \Delta r^2\rangle$ is the two-dimensional ($d = 2$) ensemble-averaged mean-squared displacement (MSD) of the particles undergoing Brownian motion over time, τ.[36,37]

Bulk rheology can be inferred from the passive bead trajectories using the real and imaginary components of the

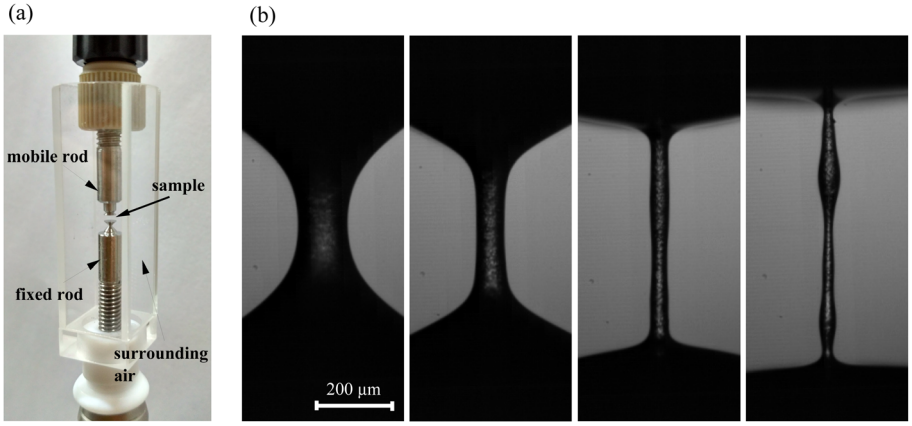

Fig. 5 (a) Detailed view of the test cell used for the uniaxial extensional rheology measurements, exactly the same configuration used in Sousa *et al.*[21] for human blood. The sample was placed in between the rods with an initial gap of about 500 μm. To induce filament thinning, the slow retraction method[32] was used (at a constant velocity of 10 μm s^{-1}). (b) Sequence of images of the evolution of a filament of the particulate viscoelastic fluid DMSO/W-PEO4M$_{45:1}$, the time interval between each image is 140 μs.

frequency-dependent complex shear modulus $G^* = G' + iG''$ and Euler's formula with

$$G^*(\omega) \sim \frac{dkT\exp[i\pi\alpha(1/\omega)/2]}{3\pi a\langle\Delta r^2(1/\omega)\rangle\Gamma[1+\alpha(1/\omega)]}, \quad (4)$$

where Γ designates the gamma function, $\omega = 1/\tau$ is angular frequency and α is the logarithmic slope assumed for the MSD.[38]

Monodisperse PMMA microspheres with (nominal) radius $a = 3$ μm are added to the fluids at a concentration of 0.05% (w/w) and used as tracer particles (Spheromers CA6, Microbeads AS). MPT microrheology measurements are taken for each equilibrated solution (sample volumes of roughly 260 μl) pipetted into the sample chamber (137-1-40, Hellma Analytics). The openings of the chamber are then sealed to prevent the sample from being in contact with ambient air and, therefore, avoid bulk flow (or drift) and/or evaporation. Particle motion was observed at room temperature (19.4 ± 0.2 °C), resulting in a reference fluid temperature ($T_{ref} \sim 20$ °C) inside the chamber of 20.8 ± 0.3 °C. Bright-field optical video microscopy with a high-speed CMOS camera (FASTCAM UX100, Photron) is used to capture the movement of the probe particles at 63× magnification using an inverted microscope (DM IL LED, Leica). Data are collected at $f = 125$ fps and $\phi = 8$ ms exposure time for 3750 frames (30 s). The probe positions are tracked by an image processing algorithm and two-dimensional particle trajectories are formed by linking the probes found in consecutive video frames.[39] Data were taken at different positions in each sample to check them for spatial heterogeneity—*i.e.* ensure that rheological properties do not vary spatially—and de-drifted (convective drift and vibration can introduce errors).[40] The MSD values were calculated at various lag times using unbiased estimates derived elsewhere.[41] The apparent motion of immobilised tracer particles was measured to determine the noise floor and a resolution of about 10^{-4} μm^2 in $\langle\Delta r^2\rangle$ was obtained, which was used to correct the estimated MSD of the probes for static errors from camera noise.[22,42]

3 Results and discussion

3.1 Morphology and mechanical properties of the microparticles

Fig. 6 shows the DI at the nozzle neck for PDMS particles fabricated with different ratios of the precursors and for healthy RBCs. The PDMS precursors ratio (% wt, siloxane base to curing agent) was varied from the standard 10 : 1 to 60 : 1. Above the latest ratio, the material did not crosslink and remained as a highly viscous liquid. The observed deformability increased with the ratio, and became close to that of the RBCs for the larger ones.

Fig. 7 shows the correlation between the deformation index and the elastic modulus. The dotted line indicates a possible potential fit line for PDMS particles to predict the relationship between both parameters for the measurements in a micronozzle with a neck diameter of 66 ± 3 μm and a Q of 5 μl min^{-1}, under the conditions mentioned in López *et al.*[13] The elastic modulus reported for the largest ratio is also close to that of RBCs. Finally, Fig. 8 compares the size of the RBCs and that of the PDMS particles for 45 : 1 and 60 : 1 ratios. The bars represent the probability distribution of the RBCs' larger dimension D_{RBC}(red) and the particle diameter D_p(grey). The mean size of the particle for both ratios matches with that previously reported for the particle fabrication method for lower ratios.[13] However, there is a significant higher heterogeneity in size for 60 : 1 than the 30% reported for this particle fabrication method using lower precursor ratios,[13] probably because of the crosslinking disparity due to the low proportion of the curing agent. Nevertheless, these results show that PDMS particles fabricated with 45 : 1 or 60 : 1 ratios may be adequate candidates for mimicking RBCs' deformability and, hence, to develop viscoelastic particulate blood analogues.

3.2 Shear rheology

The steady shear viscosity of the viscoelastic base solutions for different PEO molecular weights M_w is shown in Fig. 9(a). In

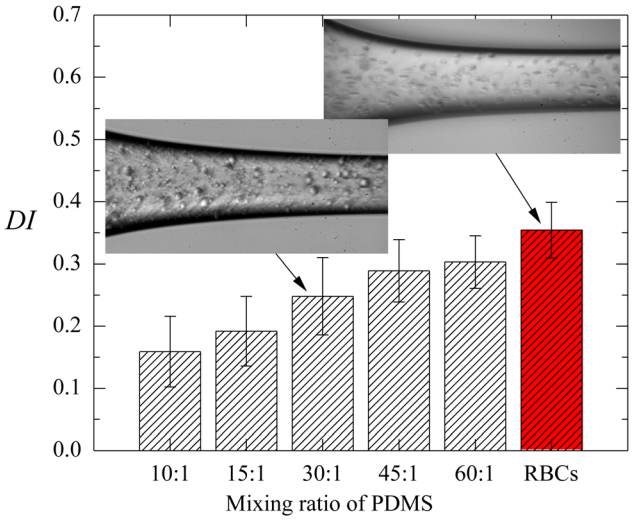

Fig. 6 Deformation index of PDMS particles produced with different precursor ratios (Part A : Part B) and healthy RBCs. The insets show images of PDMS particles (30 : 1) and RBCs flowing through our micronozzles.

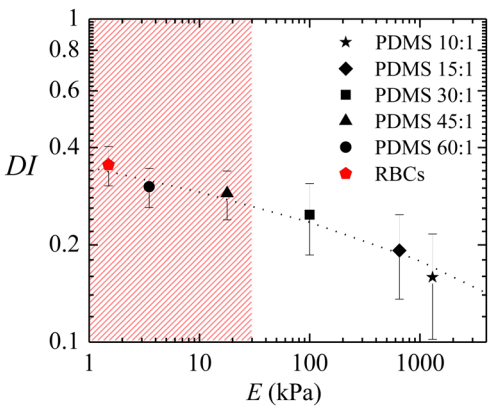

Fig. 7 Deformation index DI of PDMS particles produced with different precursor ratios (Part A : Part B) and human healthy RBCs *versus* the literature elastic modulus *E*. The red symbol corresponds to the most accepted value for the mean elastic modulus *E* of RBCs and the red striped region points out the range of *E* values for human RBCs in the literature. The dotted line shows a possible fitting to the PDMS particle values.

general, all samples present an almost constant viscosity in agreement with the dilute regime of the PEO solutions prepared.[43] The viscosity value observed at high shear rates (η_∞), varies slightly from 1.33 ± 0.01 mPa s to 1.42 ± 0.01 mPa s, corresponding to the solutions with 50 ppm of PEO of 600 kDa and 8 MDa, respectively. It is the sample prepared with PEO with the lowest molecular weight that is able to match the value of the estimated zero shear viscosity, η_0, obtained for human blood plasma at 37 °C by Brust *et al.*[20] with a value of 1.34 mPa s (shown as grey line in Fig. 9a).

When 42 vol% of the fabricated PDMS particles with different PDMS mixing ratios, corresponding to the particles with similar DI to that of RBCs (PDMS 30 : 1, 45 : 1 and 60 : 1), are added to the base viscoelastic solution DMSO/W-PEO8M, the viscosity values increased, and also a shear-thinning behaviour (a decrease of viscosity as a function of shear rate) can be observed for all samples as a result of the initial aggregation and consequent disaggregation of the PDMS particles during flow [Fig. 9(b)]. The mechanism responsible for the shear-thinning behaviour has motivated many studies in the last few decades on several systems as Brownian colloidal suspensions and non-Brownian suspensions, and for rigid and less rigid microparticles. The shear-thinning behaviour of our suspensions (in the limit of non-Brownian suspensions) could be mainly caused by the presence of adhesive forces between particles, as reported by Gilbert *et al.*[45] in their study on PDMS suspensions. When these adhesive forces are presented, the shear-thinning behaviour appears because of the formation of agglomerates that break down when the deformation is increased, leading to a reduction of these structures into units and thus decreasing the viscosity with the shear rate,[46] as in the case of blood. Nevertheless, the value of the viscosity and the degree of shear-thinning is different according to the deformation index of the particles. The highest values of the viscosity at low shear rates correspond to the solution with less deformable particles (a PDMS precursor mixing ratio of 30 : 1), maybe related to the fact that these particle are able to resist more the shear stress leading to a disturbance flow that increases the viscous dissipation rate.[47,48]

To further understand these results, the ratio between viscous and elastic forces, denoted as the capillary number Ca, which is the most important dimensionless number that takes into account the deformability of the particles, was analysed. The capillary number Ca can be written as follows:

$$\mathrm{Ca} = \frac{\sigma}{E}, \tag{5}$$

where σ is the shear stress and E the elastic modulus of the particles.[49]

Under flow, high values of Ca mean that particles are more sensitive to the variation of the shear rate leading to a change in their shape.[50]

The highest Ca corresponds to samples with particles with a mixing PDMS ratio of 60 : 1 ($\mathrm{Ca}^{60:1} > \mathrm{Ca}^{45:1} > \mathrm{Ca}^{30:1}$). The ability to better deform provokes a higher number of particles to migrate to the area where the shear rate is low, and as a result the viscosity of the suspension decreases in comparison with that of the samples with particles of lower mixing ratios.

Moreover, Fig. 9(b) allows one to check the effect of the viscoelastic base solution (potential plasma analogue) on the shear viscosity results; as can be observed, the curves for DMSO/W-PEO8M$_{45:1}$ and DMSO/W-PEO4M$_{45:1}$ practically overlap. The presented results indicate that shear rheology depends mostly on the PDMS mixing ratio of the particles, rather than on PEO molecular weight.

The shear viscosity curve for the whole human blood[44] is also presented in Fig. 9(b). For a wide range of shear rates, the base viscoelastic solution with PDMS particles of ratio 45 : 1 seems to match reasonably with that of the real human blood. Nevertheless, even when the viscous behaviour showed in the

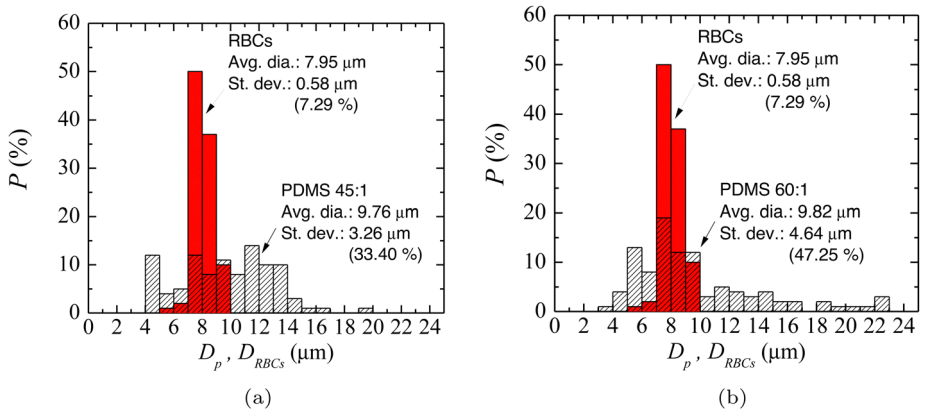

Fig. 8 Probability distribution of the resting size of healthy RBCs $P(D_{RBC})$ (red bars) and PDMS particles $P(D_p)$ fabricated with the precursor ratios, part A : part B, 45 : 1 (a) and 60 : 1 (b) (striped bars).

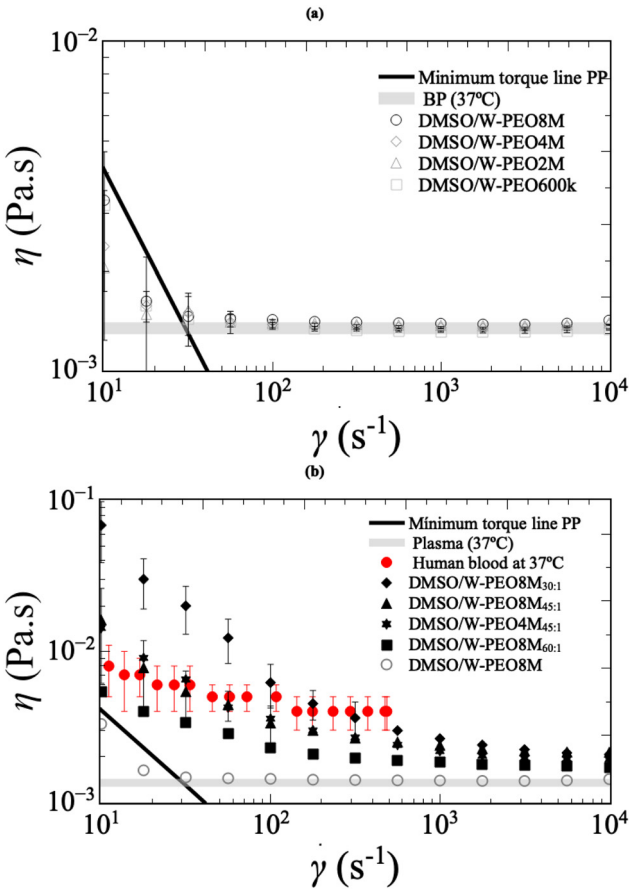

Fig. 9 Steady shear viscosity curves at 20 °C. (a) Viscoelastic base solutions at different molecular weights of PEO in comparison with the viscosity of human blood plasma at 37 °C Brust *et al.*,[20] (b) shear viscosity for the viscoelastic base solution (DMSO/W-PEO8M) and the particulate viscoelastic solution with different PDMS mixing ratios of the added particles in comparison with the viscosity of human blood at 37 °C.[44]

viscosity curves is close to the viscous behaviour of human blood, the elastic contribution cannot be underestimated. In the following sections, uniaxial extensional flow and microrheology experiments will be discussed to understand the elastic behaviour of the working fluids to be compared to that of the human blood and human blood plasma.

3.3 Extensional relaxation times

Fig. 10 depicts the extensional relaxation time λ_e as a function of molecular weight M_w of the polymer (PEO) used in our working fluids (see Table 1). The results are compared to those of human plasma and blood from the literature, at 37 °C[20] and 21 °C.[21] Note that the very weak viscoelastic character of human plasma/blood obtained in Sousa *et al.*[21] contrasts with the previous observations in Brust *et al.*[20] The different experimental conditions, such as the concentration of anticoagulant used in blood collection may explain these significant differences according to Sousa *et al.*[21] The results in Fig. 10 exhibit a power law dependence of λ_e on the molecular weight M_w, in agreement with the previous studies on other polymeric solutions.[51,52] Moreover, the addition of the PDMS microparticles (around 42 vol%) to the plasma analogues does not modify

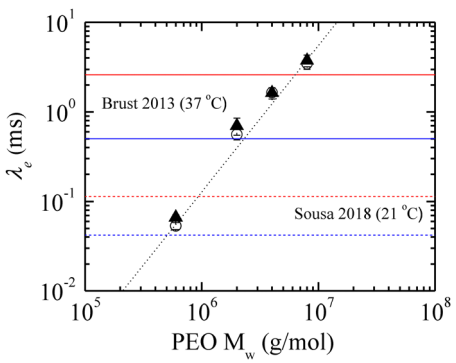

Fig. 10 Extensional relaxation time λ_e *versus* M_w of the PEO used. Viscoelastic base solutions (white circles) and particulated viscoelastic solutions (around 42% by volume of particles, black triangles). Lines depict the results of the extensional relaxation time for human plasma (blue) and whole blood (red), from Brust *et al.*[20] (solid line) and Sousa *et al.*[21] (dash line). The experiments were conducted in air, at 22 ± 2 °C. The dot line is the fitting $\lambda_e = 2 \times 10^{-11} M_w^{1.6342}$ to the experimental results without particles (with λ_e and M_w measured in ms and g mol^{-1}, respectively).

substantially the results of λ_e without particles, different from what actually happens between plasma and whole blood, where RBCs contributed clearly to the increase of λ_e. Particles with RBC-like morphology may behave differently from their spherical counterparts concerning their physical performances (attachment, adhesion performance, orientation, *etc.*) giving rise to this different behaviour under an extensional flow.

As can be observed, the viscoelastic fluids prepared with a PEO of M_w = 4 MDa (4×10^6 g mol^{-1}) show the best agreement with the results for human plasma and blood presented in Brust *et al.*[20] However, the working fluids with a PEO of M_w = 600 kDa (6×10^5 g mol^{-1}) match better with the results from Sousa *et al.*[21] In spite of the different time scale and temperature, the breakup of the solution DMSO/W-PEO4M$_{45:1}$, previously showed in Fig. 5(b), is similar to that of human whole blood in Sousa *et al.*[21] Therefore, the elasticity of the plasma and blood analogue fluids is tunable by means of the addition of PEO with a suitable M_w, allowing elasticity to be adapted for special cases, for example, the variation of the haematocrit due to sickness.[53]

3.4 Linear viscoelasticity

The diffusive behaviour of the polymer solutions (or plasma analogues) with increasing PEO molecular weight M_w was studied by quantifying the random walk dynamics of embedded colloidal probe beads, characterised by the ensemble-averaged MSD, *i.e.*, a time-dependent quantity related to the diffusion coefficient D by $\langle \Delta r^2 \rangle = 2dD\tau$ in a Newtonian fluid [Fig. 11(a)]. At short timescales, the motion of the particles is sub-diffusive—*i.e.*, the hallmark of viscoelastic behaviour—with power-law exponents lower than unity, consistent with the values of longest relaxation time λ_e determined under uniaxial extensional flow: $\alpha_{8M} < \alpha_{4M} < \alpha_{2M} < \alpha_{600K} < 1$. The elastic response is due to the relaxation of the polymers in solution. With increasing PEO molecular weight the MSD decreases and the range of times with a sub-diffusive scaling exponent ($\alpha < 1$) becomes slightly wider, since the polymer coils take a longer time to relax. The slope of the MSD then exhibits a crossover to diffusive behaviour as it increases to reach a value of unity ($\alpha \to 1$). At longer times, away from the noise floor, the MSDs exhibit a linear trend as a function of lag time ($\alpha = 1$), indicating that the motion of the tracer particles is purely diffusive

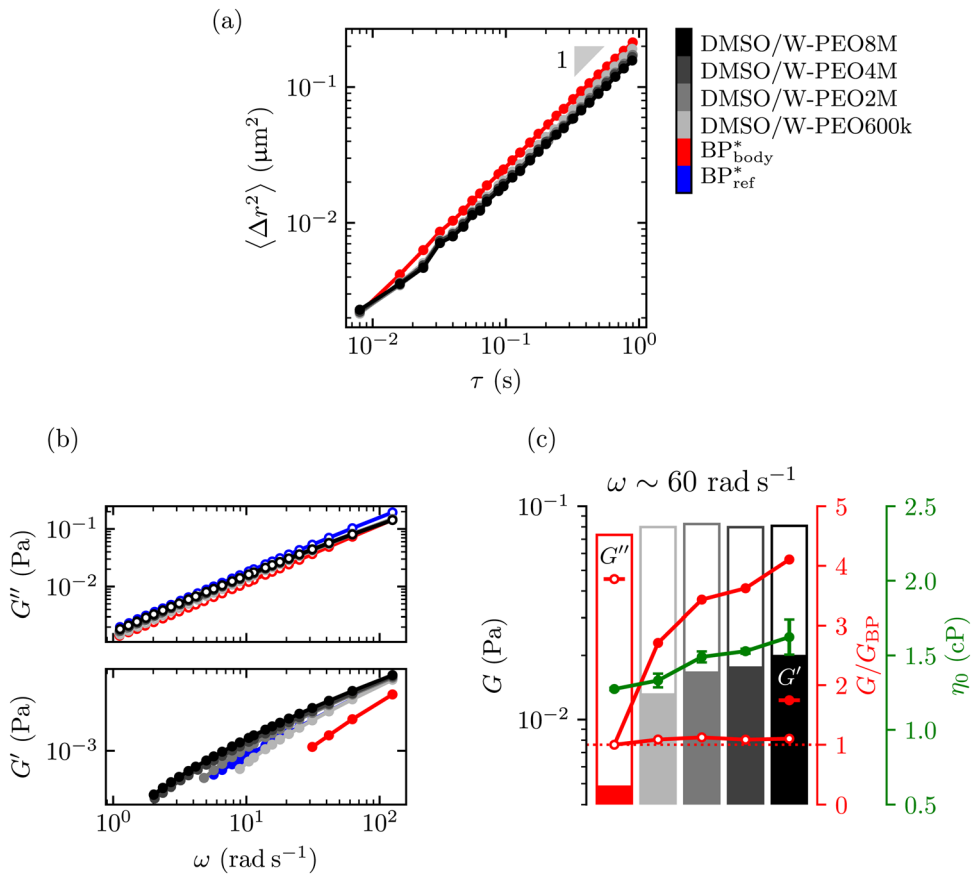

Fig. 11 Linear rheological response obtained from MPT microrheology for particles moving in artificial and (*) native blood plasma (BP).[22] (a) Ensemble-averaged MSD as a function of lag time τ. The slope marker indicates the scaling $\langle \Delta r^2 \rangle \propto \tau$ at the purely viscous long-time limit of the MSDs. Error bars are not shown on MSD plots for clarity. The noise floor is roughly 10^{-4} μm^2 (not shown). Increasing PEO molecular weight results in decreased MSD of particles. (b) Real and imaginary parts of the inferred complex shear moduli G^* (lower and upper plots, respectively) by comparison with human plasma at 37 and 20 °C (red and blue datasets, respectively). (c) Comparison of absolute (black leftmost axis) and scaled (red middle axis) shear moduli at a fixed frequency ($\omega \sim 60$ rad s^{-1}), and viscosity (green rightmost axis). Increasing PEO molecular weight results in increased viscosity and shear-thinning behaviour.

and the microenvironment surrounding them responds like a viscous (or Newtonian) fluid. At such long timescales, particles are able to diffuse through the molecular network at rates limited by the viscosity η_0 of the complex fluid: $\eta_0^{8M} > \eta_0^{4M} > \eta_0^{2M} > \eta_0^{600K}$. Here, by fitting the data to MSD = $4D\tau$ (for $d = 2$) we obtain a diffusion coefficient, which can then be used to determine the zero-shear viscosity. Ensemble-averaged van Hove correlation functions of the microspheres mixed in the polymer solutions for different values of lag time are well fit to a Gaussian (data not shown), indicating a homogeneous environment.[54]

Fig. 11(b) shows the viscoelastic moduli G' and G'' as a function of angular frequency ω over roughly two orders of magnitude in frequency. MPT measurements have been performed in the frequency range of 1–125 rad s^{-1}, where the upper limit is given by the acquisition rate f of the camera. For all solutions and times/frequencies investigated, it was found that $G'' > G'$, *i.e.*, dissipation dominates storage in the exchange of thermal energy between the probe particles and the medium. It is worth noting that in the case of G', absolute values are in rather good agreement with those determined by Rodrigues and co-workers from MPT measurements on actual plasma at a reference temperature of about 20 °C (BP_{ref}).[22] Conversely, they seem to diverge from those obtained at body temperature (BP_{body}). This mismatch in G'—*i.e.*, in elasticity—shows that to more accurately model the frequency-dependent linear viscoelastic properties of human blood plasma at 37 °C (body temperature) a slightly lower PEO molecular weight and/or concentration should suffice, with little to no solvent tweaking required (namely of the DMSO–water mixture) in light of the quantitative agreement in G'' already expected from the viscosity curves. Such an agreement becomes more apparent by plotting G''/G''_{BP} at a given frequency [Fig. 11(c), red middle axis], with values approaching unity (dotted line) for all PEO molecular weights. The zero-shear viscosity η_0 of the polymer solutions has been determined using a wall-effect corrected form of the classic Stokes–Einstein equation evaluated at the purely viscous long-time slope ($\tau \sim 1$ s) of the MSDs [Fig. 11(c), green rightmost axis].[22] At about 1.5 times that of water, the viscosity values obtained from MPT microrheology are consistent with steady shear rheology using a rotational rheometer. The specific viscosity $\eta_{sp} = \eta_0/\eta_s - 1$ scales as $\eta_{sp} \propto M_w^{0.57\pm0.16}$, where $\eta_s \sim 1.30$ cP is the solvent viscosity (at 20 °C) and the exponent is obtained from a power-law fit to the data (not shown). All in all, a general qualitative agreement is found between the frequency behaviour of the four PEO solutions formulated and that reported in the literature for native blood plasma.[22] As far as matching the linear viscoelastic response of the biofluid at body temperature goes, the moduli of the M_w = 600 kDa PEO solution make it the best candidate for a rheological analogue; this is in line with the shear viscosity measurements [Fig. 9(a)]. Bear in mind, though, that different relaxation times have been reported for blood plasma, possibly a consequence of the ratio and type of anticoagulant used in the blood collection[20,21] (see also Fig. 10).

3.5 Cell-free layer (CFL) in a microfluidic channel

As previously mentioned, the use of microparticles in blood analogue fluids has been demonstrated to be essential to reproduce multiphase effects taking place in the human microcirculatory system, such as the cell-free layer (CFL) phenomena. The flow of the plasma analogue fluid (DMSO/W-PEO4M) with a 20% by volume of PDMS microparticles (45 : 1) was analyzed through a microfluidic channel with an important constriction, to simulate a microstenosis, and the results were compared with those of human blood,[55] also with a concentration of 20% by volume of RBCs. Fig. 12-a shows the design of the microfluidic device used in this study, the same as that used in Rodíguez-Villarreal *et al.*[55] to study the effect of temperature and the flow rate on the cell-free area. For the flow rates (Q) used in the *in vitro* experiments, this geometry gave rise to a high shear rate of around 10^4 s^{-1}, and allowed one to get a wide free layer of particles due to the flow inertia. RBCs are subjected to similar shear rates under physiological conditions in the smallest and atherosclerotic arteries.[56] Images of the flow in the interest area (red rectangle) were taken by using a high-speed camera (Photron, Fastcam Mini UX50) equipped with the corresponding lenses and an optical fibre light source. During the flow experiments through our PDMS microchannel (microstenosis), sedimentation was not observed, but the contraction was partially blocked after around ten minutes in most of the experimental runs. Please, note that the concentration of particles is relatively high for this type of CFL studies (see ref. 1 and references therein).

Fig. 12 shows the results for RBCs suspended in plasma [Fig. 12(b)][55] and PDMS (ratio 45 : 1) particles in the plasma analogue (DMSO/W-PEO4M) [Fig. 12(c) and (d)]. The solid lines in (c) point out the free area of particles with diameters higher than 6 μm (sizes similar to RBCs). It should be noted that the size distribution $\mathcal{P}$ of our PDMS particles is much wider than that of RBCs, see Fig. 8 (left). It was more difficult to move the smallest particles (sizes similar to platelets) to the center of the stream, but most of the particles were in the area marked with the solid lines. For this reason, attention was focused on the particles with sizes similar to RBCs. The particulate blood analogue (plasma analogue + 20% of PDMS particles) exhibits a clear area or layer free of PDMS particles, showing a good agreement with the results for RBCs in plasma. At a higher flow rate Q of 12 ml h^{-1}, as expected, the particle free area increased [see Fig. 12(d)], and, in this case, a layer completely free of particles can be seen, at around 10 μm from the walls.

3.6 Droplet impact behaviour onto a solid surface

A macroscale application in the field of forensic science is also presented in this manuscript, concerning the impact of the blood analogue droplets onto a solid surface for bloodstain pattern analysis. Recently, an experimental study concluded that the use of deformable particles rather than rigid particles in blood simulants was highly recommended for better reproducibility of human blood spreading and splashing behaviour in droplet impact for bloodstain pattern analysis.[5]

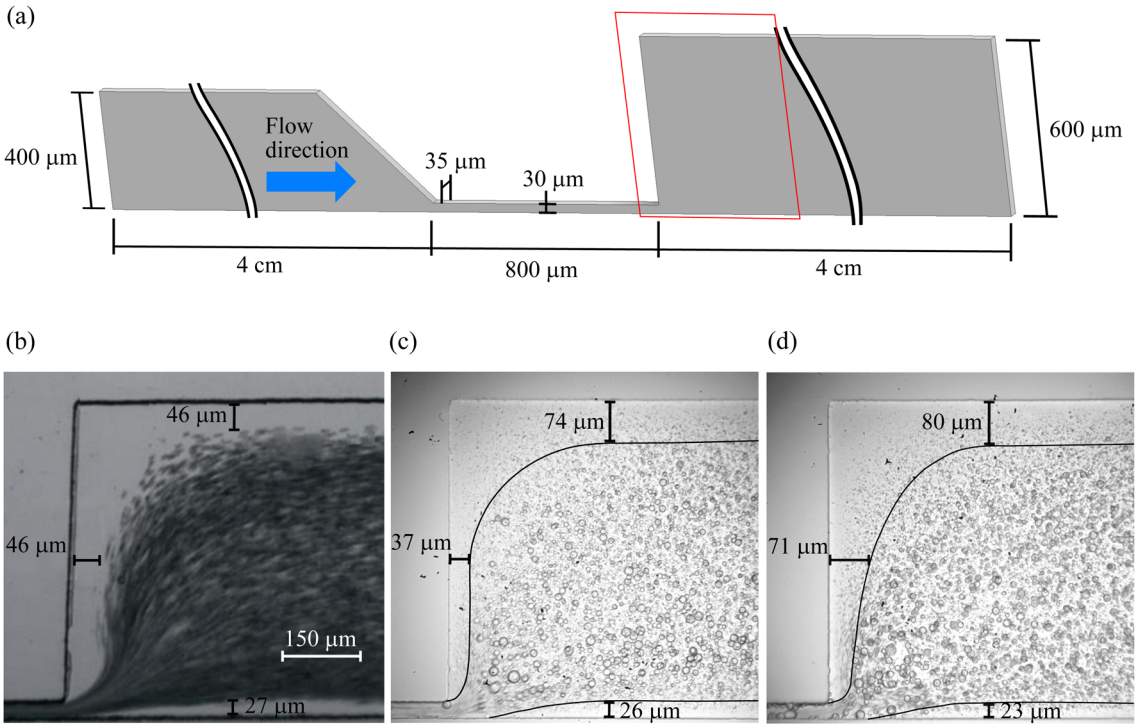

Fig. 12 Cell (particle) free layer (CFL/PFL) effect on a microfluidic channel designed from Rodíguez-Villarreal *et al.*[55] (a) Schematic representation of the microfluidic channel. The red rectangle marks the window used in the experiments (b–d). (b) Image of RBCs suspended in plasma at a concentration of 20% by volume, at 27 °C, and at a flow rate Q of 6 ml h^{-1} [55] (in Rodíguez-Villarreal *et al.*,[55] results at 27 and 37 °C were similar). (c and d) Images of PDMS 45 : 1 particles in the plasma analogue DMSO/W-PEO4M at a concentration of around 20% by volume, at room temperature, and at Q = 6 and 12 ml h^{-1}, respectively. The solid lines in (c) and (d) are a guide to the eye, marking the free area of particles with diameters higher than 6 μm (sizes similar to RBCs). Figure (b) is reproduced from Rodíguez-Villarreal *et al.*[55] with permission from MDPI.

Following the experimental procedure described in Yokoyama *et al.*,[5] experiments of droplet impact of the proposed blood analogue DMSO/W-PEO4$M_{45:1}$ were conducted. The results were compared to those of dog blood (similar to human blood).[5] It should be noted that the blood analogue fluid has been developed to match the blood properties at 37 °C (body temperature) while it is used at room temperature, whereas, in the literature related to this field, the impact of blood droplets is studied at 20 °C. Thus, the physical blood properties vary considerably, specially viscosity, and therefore Reynolds number (Re). In fact, the cooling of blood drops in flight and during impact has never been addressed in the context of bloodstain patterns analysis.[57] Drop in-flight atomization, impact spreading and splashing should be affected by the temperature of the fluid, and probably, in most of the cases, the temperature might be near 37 rather than 20 °C, because the spatter originates from blood at body temperature, but this issue is out of the scope of this work.

Briefly, the proposed blood analogue fluid was injected slowly through a steel capillary (1.27 mm in outer diameter) forming a pendant drop that eventually detached under its own weight. The capillary could be displaced along a vertical support to control the height over the target substrate, and consequently the normal impact velocity V (between 2 and 4 m s^{-1}). The target substrate consists of a clean glass slide with a typical root-mean-square roughness of a few nanometres. Bottom-view and side-view images of the drop impact were taken by using a high-speed camera (Photron, Fastcam SA5) at 10 000 and 150 000 frames per second, respectively. More details of the experimental procedure can be found in Yokoyama *et al.*[5] Fig. 13 shows the good agreement for the evolution of the spreading radius R_t of dog whole blood[5] and that of the blood particulate analogue fluid DMSO/W-PEO4$M_{45:1}$ for Weber number, We, around 200; We = $\rho R_0 V^2/\gamma$, where ρ is the density, R_0 the initial radius of the impacting drop, V

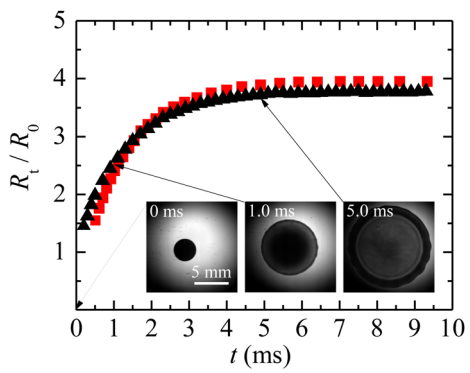

Fig. 13 Time evolution of spreading radius R_t of dog whole blood (red squares,[5]) and the blood particulate analogue fluid DMSO/W-PEO4$M_{45:1}$ (black triangles), with We around 200 in both cases; t = 0 is the time at which the droplet contacts the solid surface. The insets are bottom-view images of the impacting droplet at different times.

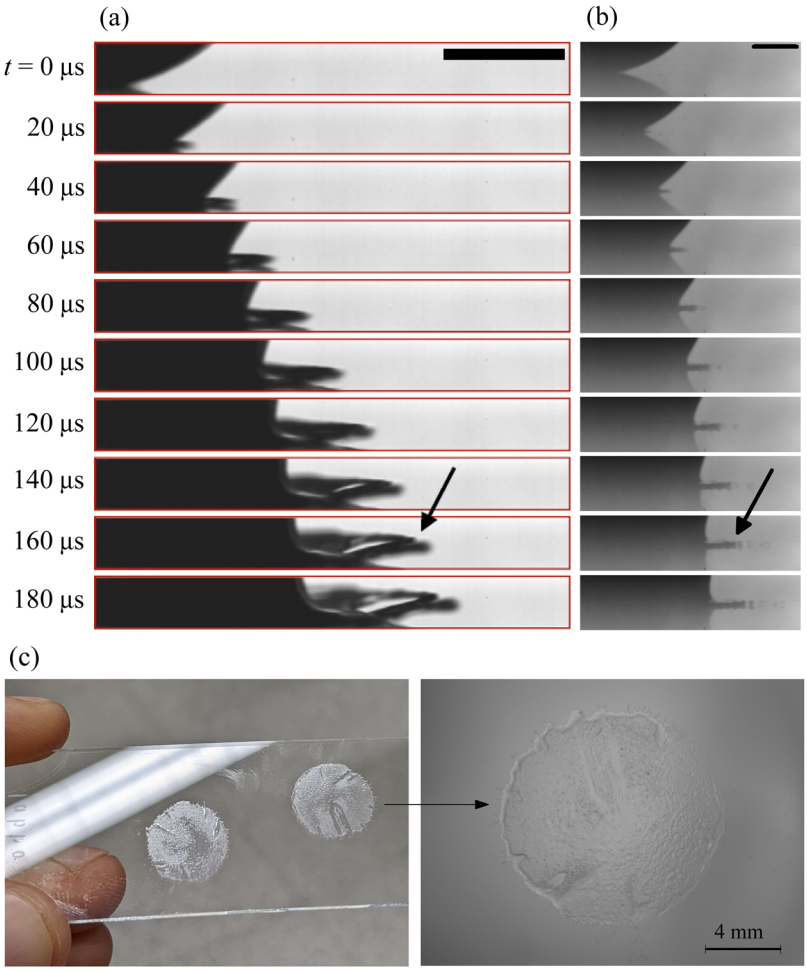

Fig. 14 Side-view images of impacting droplets of dog whole blood (a), from Yokoyama *et al.*,[5] and our blood particulate analogue fluid DMSO/W-PEO4M$_{45:1}$ (b), at a We around 600. The arrows point out the splashing. The scale bar in (a and b) corresponds to 1 mm. (c) Images of the dry stain, after the evaporation of the analogue plasma, for bloodstain pattern analysis. Figure (a) is reproduced from Yokoyama *et al.*[5] with permission from Elsevier.

the normal velocity of impact of the drop, and γ the surface tension. A crucial parameter for reconstructing a crime scene through bloodstain pattern analysis is the spreading factor R_{max}/R_0, and the result of our blood analogue is similar to that of whole blood.

Fig. 14 compares the splashing of dog whole blood (a) from Yokoyama *et al.*[5] with that of our blood particulate analogue fluid DMSO/W-PEO4M$_{45:1}$ (b) for a higher We of around 600. In the case of real blood, a clear and typical Corona splash is observed in the images, which normally takes places for a Ohnesorge number Oh, Oh $= \mu/\sqrt{\rho R_0 \gamma}$, above 0.0062 (relatively viscous liquids).[5] The splashing of our blood analogue could be also considered as Corona splash, although without a clear lift-off of the lamella. As aforementioned, our fluid was developed to match the blood properties at 37 °C, and its Oh is around 0.008, close to the transition from Corona to prompt splash, which may explain the different behaviour between both droplet impacts. Furthermore, the transfer of momentum between particles is suppressed by the high capacity to deform of our PDMS particles (similar to RBCs) and no particle ejection was expected/obtained (tiny-splashing) different from blood simulant containing rigid particles.[5]

Our results show the potential of our developed fluid to be used as a blood simulant in forensic science, taking into account the fluid body temperature in the droplet impact for bloodstain pattern analysis; Fig. 14(b) illustrates this application.

4 Conclusions

A novel particulate blood analogue fluid able to reproduce rheological and some physiological characteristics of real human blood at body temperature was developed. The blood analogue is based on a viscoelastic solution, able to reproduce the rheological behavior of blood plasma, with deformable PDMS particles at a concentration similar to the human haematocrit. The general mechanical deformability of RBCs was captured by the intelligent fabrication of simple spherical PDMS particles, used in this work as RBC templates. The improvement of the monodispersity of these PDMS particles, while maintaining the high production rate, is desirable to match the size distribution of RBCs, and continues to be a grand challenge (see ref. 1 and references therein).

The shear rheology of the blood analogue only depends significantly on the PDMS particle composition, the solution with particles of PDMS 45 : 1 being in best agreement with the viscous behaviour of human blood. The elastic behaviour under uniaxial extensional flow of the blood analogues DMSO/W-PEO4M$_{45:1}$ and DMSO/W-PEO600K$_{45:1}$ agrees with the results of Brust *et al.*[20] and Sousa *et al.*,[21] respectively. The elasticity of the developed plasma analogue can be adjusted to the results of human plasma from Brust *et al.*[20] or Sousa *et al.*[21] by means of the addition of PEO with a suitable M_w, among other special conditions (sickness). The viscoelastic moduli of the plasma analogues obtained by means of passive microrheology are in good agreement with the results of the steady shear experiments, indicating that the DMSO/W-PEO600K solution is a fairly good candidate for mimicking the non-Newtonian behaviour of blood plasma at body temperature.

The flow of the particulate blood analogue fluid DMSO/W-PEO4M$_{45:1}$ through a narrow microchannel reproduced the CFL phenomena, showing its potential for the *in vitro* study of multiphase flow effects in the microcirculatory system. On the other hand, its application in bloodstain pattern analysis is promising and this would allow the fluid body temperature in the droplet impact to be considered, while working at room temperature.

It is worth pointing out that the developed blood analogues just present a similar rheological behavior with blood flow under certain flow conditions. The purpose of this study is to look for a replacement solution able to reproduce specific flow characteristics with the aim to understand the features found in the human circulatory system due to the viscoelastic properties of blood (microscale and confinement characteristics) and/or for other technical purposes as the analysis of some patterns due to a blood drop impact (macroscale without confinement). The physiological functions of these blood analogues are out of the scope of this work. Moreover, the rheological differences in terms of viscosity and elasticity can be adjusted by varying the amount of polymer and the mixing ratios of the solvent, as well as the concentration of the PDMS particles to adjust them to any specific situation (temperature, level of hematocrit, *etc.*). Nevertheless, any comparison with real blood flow has to be made with criticism as many rheological characteristics of blood such as thixotropy of yield stress are even not reproduced in these analogues.

Author contributions

E. J. V. and L. C. D.: conceptualization, formal analysis, writing, reviewing, editing, funding acquisition and supervision; A. R.: experimental data and writing; M. L.: experimental data; T. R.: multiple particle tracking data and writing.

Conflicts of interest

There are no conflicts to declare.

Acknowledgements

We thank Samir Sadek for insightful discussions and help with experiments. A. R., M. L. and E. J. V. gratefully acknowledge the support of the Spanish Ministry of Science and Education (grant no. PID2019-108278RB-C32/AEI/10.13039/501100011033) and Gobierno de Extremadura (grants no. GR21091 and IB18005, partially supported through FEDER). TR and LCD acknowledge FEDER (COMPETE 2020 and NORTE 2020), FCT/MCTES (PIDDAC) and FCT for funding support under grants no. PTDC/EME-EME/30764/2017, PTDC/EME-APL/3805/2021, 2021.06532.BD, LA/P/0045/2020, UIDB/00532/2020, UIDP/00532/2020 and NORTE-01-0145-FEDER-000054.

References

1 S. H. Sadek, M. Rubio, R. Lima and E. J. Vega, Blood particulate analogue fluids: A review, *Materials*, 2021, **14**, 2451.
2 M. Belenkovich, J. Sznitman and N. Korin, Micro-particle entrapment dynamics in microfluidic pulmonary capillary networks, *J. Biomech.*, 2022, **137**, 111082.
3 N. Doshi, A. S. Zahr, S. Bhaskar, J. Lahann and S. Mitragotri, Red blood cell-mimicking synthetic biomaterial particles, *Proc. Natl. Acad. Sci. U. S. A.*, 2009, **106**, 21495–21499.
4 C. L. Modery-Pawlowski, L. L. Tian, V. Pan and A. Sen Gupta, Synthetic approaches to rbc mimicry and oxygen carrier systems, *Biomacromolecules*, 2013, **14**, 939–948. PMID: 23452431.
5 Y. Yokoyama, A. Tanaka and Y. Tagawa, Droplet impact of blood and blood simulants on a solid surface: Effect of the deformability of red blood cells and the elasticity of plasma, *Forensic Sci. Int.*, 2021, **331**, 111138.
6 G. Ciasca, M. Papi, S. Di Claudio, M. Chiarpotto, V. Palmieri, G. Maulucci, G. Nocca, C. Rossi and M. De Spirito, Mapping viscoelastic properties of healthy and pathological red blood cells at the nanoscale level, *Nanoscale*, 2015, **7**, 17030–17037.
7 J. Liu, Y. Han, W. Hua, Y. Wang, G. You, P. Li, F. Liao, L. Zhao and Y. Ding, Improved flowing behaviour and gas exchange of stored red blood cells by a compound porous structure, *Artif. Cells, Nanomed., Biotechnol.*, 2019, **47**, 1888–1897.
8 S. Barns, M. A. Balanant, E. Sauret, R. Flower, S. Saha and Y. Gu, Investigation of red blood cell mechanical properties using afm indentation and coarse-grained particle method, *BioMed. Eng. OnLine*, 2017, **16**, 140.
9 I. M. Lamzin and R. Khayrullin, The quality assessment of stored red blood cells probed using atomic-force microscopy, *Anat. Res. Int.*, 2014, **2014**, 869683.
10 K. E. Bremmell, A. Evans and C. A. Prestidge, Deformation and nano-rheology of red blood cells: An afm investigation, *Colloids Surf., B*, 2006, **50**, 43–48.
11 I. Dulińska, M. Targosz, W. Strojny, M. Lekka, P. Czuba, W. Balwierz and M. Szymoński, Stiffness of normal and

pathological erythrocytes studied by means of atomic force microscopy, *J. Biochem. Biophys. Methods*, 2006, **66**, 1–11.
12 D. Pinho, B. N. Muñoz-Sánchez, C. F. Anes, E. J. Vega and R. Lima, Flexible pdms microparticles to mimic rbcs in blood particulate analogue fluids, *Mech. Res. Commun.*, 2019, **100**, 103399.
13 M. López, M. Rubio, S. H. Sadek and E. J. Vega, A simple emulsification technique for the production of micro-sized flexible powder of polydimethylsiloxane (pdms), *Powder Technol.*, 2020, **366**, 610–616.
14 J. Carneiro, R. Lima, J. B. L. M. Campos and J. M. Miranda, A microparticle blood analogue suspension matching blood rheology, *Soft Matter*, 2021, **17**, 3963–3974.
15 A. Rubio, S. Rodríguez and M. G. Cabezas, Capabilities and limitations of fire-shaping to produce glass nozzles, *Materials*, 2020, **13**, 5477.
16 L. Vilas-Boas, V. Faustino, R. Lima, J. M. Miranda, G. Minas, C. S. Veiga-Fernandes and S. Oliveira-Catarino, Assessment of the deformability and velocity of healthy and artificially impaired red blood cells in narrow polydimethylsiloxane (pdms) microchannels, *Micromachines*, 2018, **9**, 384.
17 V. Faustino, S. O. Catarino, D. Pinho, R. Lima and G. Minas, A passive microfluidic device based on crossflow filtration for cell separation measurements: a spectrophotometric characterization, *Biosensors*, 2018, **8**, 125.
18 A. Rubio, V. Faustino, M. G. Cabezas, R. Lima and E. J. Vega, Fire-shaped cylindrical glass micronozzles to measure cell deformability, *J. Micromech. Microeng.*, 2019, **29**, 105001.
19 R. G. Lebel and D. A. I. Goring, Density, viscosity, refractive index, and hygroscopicity of mixtures of water and dimethyl sulfoxide, *J. Chem. Eng.*, 1962, **7**, 100–101.
20 M. Brust, C. Schaefer, R. Doerr, L. Pan, M. Garcia, P. E. Arratia and C. Wagner, Rheology of Human Blood Plasma: Viscoelastic Versus Newtonian Behavior, *Phys. Rev. Lett.*, 2013, **110**, 078305.
21 P. C. Sousa, R. Vaz, A. Cerejo, M. S. N. Oliveira, M. A. Alves and F. T. Pinho, Rheological behavior of human blood in uniaxial extensional flow, *J. Rheol.*, 2018, **62**, 447–456.
22 T. Rodrigues, R. Mota, L. Gales and L. Campo-Deaño, Understanding the complex rheology of human blood plasma, *J. Rheol.*, 2022, **66**, 761–774.
23 T. Kenner, The measurement of blood density and its meaning, *Basic Res. Cardiol.*, 1989, **84**, 111–124.
24 H. Hocheng, C. M. Chen, Y. C. Chou and C. H. Lin, Study of novel electrical routing and integrated packaging on biocompatible flexible substrates, *Microsyst. Technol.*, 2010, **16**, 423–430.
25 C. Ferrera, J. M. Montanero and M. G. Cabezas, An analysis of the sensitivity of pendant drops and liquid bridges to measure the interfacial tension, *Meas. Sci. Technol.*, 2007, **18**, 3713–3723.
26 J. Rosina, E. Kvašňák, D. Šuta, H. Kolářová, J. Málek and L. Krajči, Temperature dependence of blood surface tension, *Physiol. Res.*, 2007, **56**(suppl. 1), S93–S98.
27 S. S. Yadav, B. S. Sikarwar, P. Ranjan, R. Janardhanan and A. Goyal, Surface tension measurement of normal human blood samples by pendant drop method, *J. Med. Eng. Technol.*, 2020, **44**, 227–236.
28 T. Rodrigues, F. J. Galindo-Rosales and L. Campo-Deaño, Haemodynamics around confined microscopic cylinders, *J. Non-Newton. Fluid Mech.*, 2020, **286**, 104406.
29 P. C. Sousa, J. Carneiro, R. Vaz, A. Cerejo, F. T. Pinho, M. A. Alves and M. S. N. Oliveira, Shear viscosity and nonlinear behavior of whole blood under large amplitude oscillatory shear, *Biorheology*, 2013, **50**, 269–282.
30 E. D. Coninck, F. H. Marchesini, V. Vanhoorne, T. D. Beer and C. Vervaet, Viscosity of api/fatty acid suspensions: Pitfalls during analysis, *Int. J. Pharm.*, 2020, **584**, 119447.
31 P. C. Sousa, E. J. Vega, R. G. Sousa, J. M. Montanero and M. A. Alves, Measurement of relaxation times in extensional flow of weakly viscoelastic polymer solutions, *Rheol. Acta*, 2017, **56**, 11–20.
32 L. Campo-Deaño and C. Clasen, The slow retraction method (SRM) for the determination of ultra-short relaxation times in capillary breakup extensional rheometry experiments, *J. Non-Newtonian Fluid Mech.*, 2010, **165**, 1688–1699.
33 C. Ferrera, M. G. Cabezas and J. M. Montanero, An experimental analysis of the linear vibration of axisymmetric liquid bridges, *Phys. Fluids*, 2006, **18**, 082105.
34 E. J. Vega, J. M. Montanero and J. Fernández, On the precision of optical imaging to study free surface dynamics at high frame rates, *Exp. Fluids*, 2009, **47**, 251–261.
35 A. V. Bazilevsky, V. M. Entov and A. N. Rozhkov, Liquid filament microrheometer and some of its applications, *Proocedings of Third European Rheology Conference and Golden Jubilee Meeting of the British Society of Rheology*, 1990, vol. 1, pp. 41–43.
36 T. A. Waigh, Microrheology of complex fluids, *Rep. Prog. Phys.*, 2005, **68**, 685–742.
37 T. G. Mason and D. A. Weitz, Optical Measurements of Frequency-Dependent Linear Viscoelastic Moduli of Complex Fluids, *Phys. Rev. Lett.*, 1995, **74**, 1250–1253.
38 T. G. Mason, Estimating the viscoelastic moduli of complex fluids using the generalized Stokes–Einstein equation, *Rheol. Acta*, 2000, **39**, 371–378.
39 J. C. Crocker and D. G. Grier, Methods of Digital Video Microscopy for Colloidal Studies, *J. Colloid Interface Sci.*, 1996, **179**, 298–310.
40 E. M. Furst and T. M. Squires, *Microrheology*, Oxford Univ. Press, New York, US, 2017.
41 T. Savin and P. S. Doyle, Statistical and sampling issues when using multiple particle tracking, *Phys. Rev. E: Stat., Nonlinear, Soft Matter Phys.*, 2007, **76**, 021501.
42 T. Savin and P. S. Doyle, Static and Dynamic Errors in Particle Tracking Microrheology, *Biophys. J.*, 2005, **88**, 623–638.
43 K. W. Ebagninin, A. Benchabane and K. Bekkour, Rheological characterization of poly(ethylene oxide) solutions of different molecular weights, *J. Colloid Interface Sci.*, 2009, **336**, 360–367.
44 A. Z. Valant, L. Žiberna, Y. Papaharilaou, A. Anayiotos and G. C. Georgiou, The influence of temperature on rheological

properties of blood mixtures with different volume expanders—implications in numerical arterial hemodynamics simulations, *Rheol. Acta*, 2011, **50**, 389–402.
45 D. Gilbert, R. Valette and E. Lemaire, Impact of particle stiffness on shear-thinning of non-brownian suspensions, *J. Rheol.*, 2022, **66**, 161–176.
46 A. Papadopoulou, J. J. Gillissen, H. J. Wilson, M. K. Tiwari and S. Balabani, On the shear thinning of non-brownian suspensions: Friction or adhesion?, *J. Non-Newton. Fluid Mech.*, 2020, **281**, 104298.
47 M. Maleki, Rheology and migration of deformable particles in dense suspensions, *Classical Physics*, [physics.class-ph], PhD thesis, Université Grenoble Alpes, 2021.
48 M. M. Villone and P. L. Maffettone, Dynamics, rheology, and applications of elastic deformable particle suspensions: a review, *Rheol. Acta*, 2019, **58**, 109–130.
49 D. Gilbert, R. Valette and E. Lemaire, Impact of particle stiffness on shear-thinning of non-brownian suspensions, *J. Rheol.*, 2022, **66**, 161–176.
50 L. F. Chiara, M. E. Rosti, F. Picano and L. Brandt, Suspensions of deformable particles in poiseuille flows at finite inertia, *Fluid Dyn. Res.*, 2020, **52**, 065507.
51 F. Berzin, B. Vergnes and L. Delamare, Rheological behavior of controlled-rheology polypropylenes obtained by peroxide-promoted degradation during extrusion: Comparison between homopolymer and copolymer, *J. Appl. Polym. Sci.*, 2001, **80**, 1243–1252.
52 J. F. Vega, S. Rastogi, G. W. M. Peters and H. E. H. Meijer, Rheology and reptation of linear polymers. ultrahigh molecular weight chain dynamics in the melt, *J. Rheol.*, 2004, **48**, 663–678.
53 D. Pinho, L. Campo-Deaño, R. Lima and F. T. Pinho, In vitro particulate analogue fluids for experimental studies of rheological and hemorheological behavior of glucose-rich rbc suspensions, *Biomicrofluidics*, 2017, **11**, 054105.
54 M. T. Valentine, P. D. Kaplan, D. Thota, J. C. Crocker, T. Gisler, R. K. Prud'homme, M. Beck and D. A. Weitz, Investigating the microenvironments of inhomogeneous soft materials with multiple particle tracking, *Phys. Rev. E: Stat., Nonlinear, Soft Matter Phys.*, 2001, **64**, 061506.
55 A. I. Rodríguez-Villarreal, M. Carmona-Flores and J. Colomer-Farrarons, Effect of temperature and flow rate on the cell-free area in the microfluidic channel, *Membranes*, 2021, **11**, 109.
56 K. S. Sakariassen, L. L. Orning and V. T. Turitto, The impact of blood shear rate on arterial thrombus formation, *Future Sci. OA*, 2015, (1), FSO30.
57 P. M. Comiskey, A. L. Yarin, S. Kim and D. Attinger, Prediction of blood back spatter from a gunshot in bloodstain pattern analysis, *Phys. Rev. Fluid*, 2016, **1**, 043201.